Available online at www.sciencedirect.com
SCIENCE DIRECT®
Physica E 20 (2004) 338–345
PHYSICA E
www.elsevier.com/locate/physe

Ferromagnetic GaSb/Mn digital alloys

H. Luo[a,*], G.B. Kim[a], M. Cheon[a], X. Chen[a], M. Na[a], S. Wang[a], B.D. McCombe[a], X. Liu[b], Y. Sasaki[b], T. Wojtowicz[b,1], J.K. Furdyna[b], G. Boishin[c,2], L.J. Whitman[c]

[a] *Department of Physics, Center for Advanced Photonic and Electronic Materials, University at Buffalo, The State University of New York, Buffalo, NY 14260, USA*
[b] *Department of Physics, University of Notre Dame, Notre Dame, IN 46556, USA*
[c] *Naval Research Laboratory, Washington, DC 20375, USA*

Abstract

In order to realize spintronic devices in narrow-gap semiconductors, we have carried out studies on the well-known InAs/GaSb-based materials and structures. As a key component to such devices, GaSb/Mn digital alloys were successfully grown by molecular beam epitaxy. Good crystal quality was observed with transmission electron microscopy showing well-resolved Mn-containing layers and no evidence of 3D MnSb precipitates in as-grown samples. Ferromagnetism was observed in GaSb/Mn digital alloys with temperature-dependent hysteresis loops in magnetization up to 400 K (limited by the experimental setup). Magnetotransport studies were also carried out, both in the conventional Hall-bar configuration, and on gated Hall-bar structures. Both anomalous Hall effect and tunable ferromagnetism with applied gate bias were investigated. Annealing studies of the digital alloys reveal evidence of migration of Mn atoms at elevated temperatures.

PACS: 72.20; 75.50.P; 85.30.T; 72.20.My

Keywords: GaSb/Mn digital alloys; Above room temperature; Gated ferromagnetism

1. Introduction

Ferromagnetic III-Mn-V semiconductors have demonstrated their potential as a vehicle for integrating devices based on magnetic and semiconducting properties. They also promise for spin injection into semiconductor structures for new device designs [1,2]. While many studies involving ferromagnetic metal/III–V and II-Mn-VI/III–V have revealed important physics and device concepts, ferromagnetic III-Mn-V semiconductors remain a critical component in practical device applications.

In addition to being an important material system in the infrared, the unique type-II band alignments in narrow gap InAs/GaSb-based heterostructures present new opportunities in the context of spintronics. In these structures, the spatial distribution of electrons and holes can be easily controlled, which is important in controlling magnetism in the III-Mn-V materials, for which carrier-mediated exchange determines the ferromagnetism. This has been demonstrated by the successful studies of optical and electrical tuning of ferromagnetism [3,4]. While ferromagnetic GaMnAs and InMnAs exhibit well-defined hysteresis loops,

* Corresponding author.
E-mail address: luo@buffalo.edu (H. Luo).
[1] Also Polish Academy of Sciences, Al. Lotnikow 32/46, 02-668 Warsaw, Poland.
[2] Also Nova Research, Inc., Alexandria, VA 22308, USA.

1386-9477/$ - see front matter © 2003 Published by Elsevier B.V.
doi:10.1016/j.physe.2003.08.030

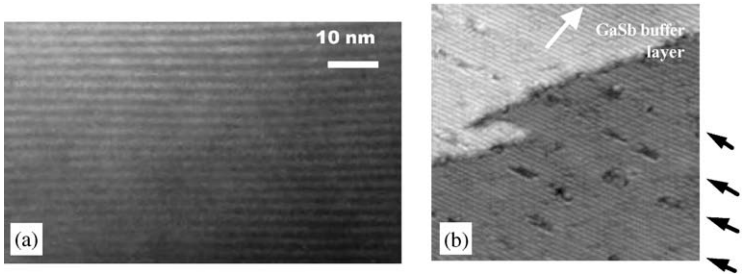

Fig. 1. (a) TEM image of a digital alloy with a repeat unit of GaSb (12 ML)/Mn (0.5 ML). The dark lines correspond to Mn-containing layers; (b) XSTM image of a GaSb (16 ML)/Mn (0.5 ML) digital alloy. The black arrows indicate the positions of the Mn-containing layers and the white arrow points to the GaSb buffer layer (opposite to the growth direction).

such clear behavior has been elusive in GaMnSb random alloys in which hysteresis loops are very small [5]. Furthermore, the Curie temperature, T_C, is low (25 K) and has to be improved for practical applications.

Theoretical calculations based on the Zener model predict room temperature ferromagnetism in GaMnN and ZnMnO for reasonable values of Mn and hole concentrations [6]. Subsequent experimental studies have showed high-temperature ferromagnetism in GaMnN, GaMnP and ZnCoO [7–9]. Room temperature ferromagnetism has also been recently observed in TiO_2 containing Co [10]. However, integration of these materials with conventional semiconductors for spintronic applications presents significant difficulties.

Our recent studies have revealed above-room-temperature ferromagnetism in GaSb/Mn digital alloys [11]. The digital alloys consist of repetitions of half a monolayer (or less) of Mn sandwiched between GaSb spacer layers of various thicknesses. The incorporation of submonolayers of Mn is expected to be in the form of randomly distributed Mn ions and MnSb islands, which is confirmed by our recent studies using cross-sectional scanning tunneling microscopy (XSTM). We will focus on our studies on GaSb/Mn digital alloys.

2. Growth and structural studies

The GaSb/Mn digital alloys were grown at a low substrate temperature (275°C) by molecular beam epitaxy (MBE) on (100) GaAs substrates. Buffer layers of GaSb (nominally 500 nm) were grown to reduce the effect of the large lattice mismatch between GaSb and the GaAs substrates (7.5%). Reflection high-energy electron diffraction (RHEED) is very effective for monitoring significant precipitation of 3D MnSb during growth. No indication of 3D precipitate formation in the RHEED patterns was observed for any of the samples used in this work. It should be pointed out that the absence of 3D MnSb precipitate formation in RHEED does not preclude the formation of such precipitates during subsequent growth. Samples for XSTM work were grown on p-type GaAs to provide the necessary electrical conductivity.

The structural properties of the materials were characterized with transmission electron microscopy (TEM), and XSTM. The TEM and XSTM images are shown in Fig. 1. The dark lines in the TEM image (Fig. 1a) are the Mn-containing layers. The TEM image shows that the overall structural quality is good, and the well-known 3D MnSb precipitates (in the NiAs structure) are absent. The XSTM image reveals the detailed distribution of Mn, showing both pseudomorphic quasi-2D islands (in the zinc-blende crystal structure) as well as randomly distributed Mn, as suggested earlier. The details of the XSTM studies will be given elsewhere [12]. Recent extended X-ray absorption fine structure (EXAFS) measurements show that the majority of Mn atoms maintain the zinc-blende bonds with post-growth annealing temperatures up to 500°C [13].

3. Magnetic properties

The magnetic properties of the samples were investigated with superconducting quantum interference device (SQUID) magnetometry and magnetotransport

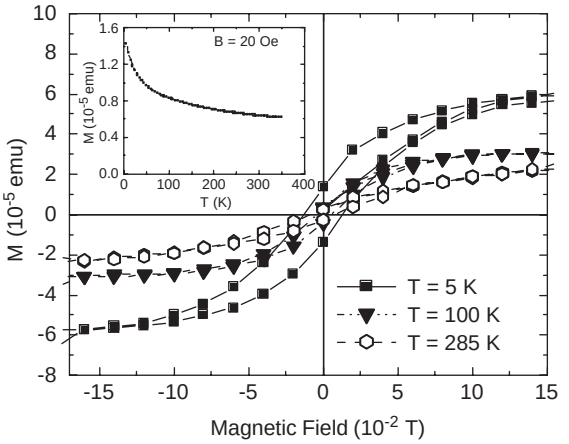

Fig. 2. Hysteresis loops of the sample shown in Fig. 1a, observed with a SQUID magnetometer, and temperature dependence of the remanent magnetization (inset).

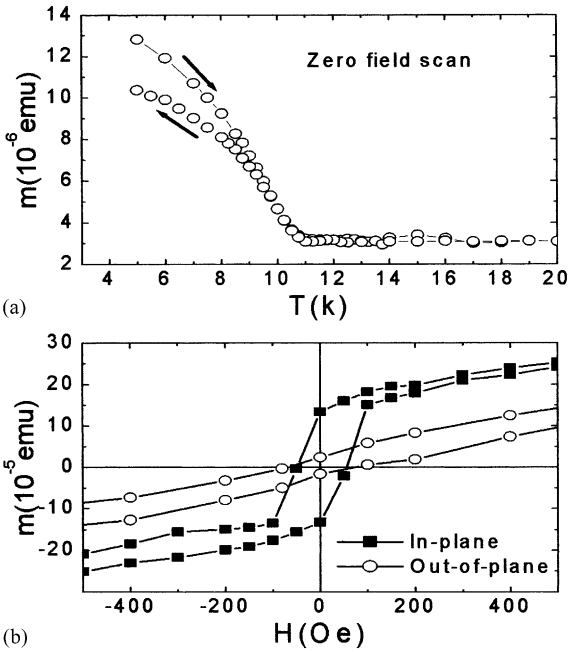

Fig. 3. (a) The temperature dependence of remanent magnetization in an as-grown GaSb 9 ML/Mn 0.5 ML digital alloy. The sample was magnetized with 3.5 T at 5 K. The up and down temperature scans were carried out after the magnet was quenched; (b) in-plane and out-of-plane hysteresis loops, which indicate an in-plane easy axis for the low-temperature ferromagnetic phase.

measurements in the Hall-bar configuration. Some of the samples showed ferromagnetism above room temperature, as indicated by hysteresis loops in the magnetization (most samples studied showed qualitatively similar magnetic behavior, and thus we show representative data for only one sample). Ferromagnetism is observed at temperatures up to 400 K (inset of Fig. 2), the upper limit of our magnetometer, and thus we can only state that $T_C > 400$ K. The hysteresis loops show clear temperature dependence over the entire range of temperatures studied, as can be seen in Fig. 2. Note that the coercive fields at 5 and 285 K are significantly different, 0.01 and 0.005 T, respectively. While ferromagnetic behavior at room temperature is also seen in GaMnAs, InMnAs and GaMnSb when there are 3D MnAs (or MnSb) precipitates, samples containing such precipitates exhibit temperature-independent hysteresis loops over a wide range of temperatures; the room temperature coercive field is nearly identical to that at 5 K. One can thus conclude from the SQUID measurements that the observed ferromagnetism in the present samples is not due to 3D MnSb precipitates. Furthermore, the shapes of the hysteresis loops for the present digital alloys differ significantly (at all temperatures) from those of MnSb precipitates in the NiAs structure [14].

Temperature-dependent magnetization data reveal additional complexity associated with the ferromagnetism in GaSb/Mn digital alloys. In the temperature dependence of the remanent magnetization, one finds an initial rapid drop with temperature at low temperatures, which changes to a slower decrease at higher temperatures. This change occurs between 30 and 50 K, as shown in the inset of Fig. 2, and suggests possible coexistence of more than one magnetic phase.

To investigate the two-phase behavior and other details of ferromagnetic properties of GaSb/Mn digital alloys, we carried out systematic studies on a GaSb 9 ML/Mn 0.5 ML, which has particularly pronounced two-phase behavior. The temperature dependence of remanent magnetization is shown in Fig. 3. In this measurement, the sample was first magnetized at 3.5 T, and the magnet was then quenched to avoid trapped field in the superconducting magnet. A Hall sensor with a detection limit of 1 Oe was used to independently probe the trapped field. The first step of the temperature scan with increasing temperature

shows a ferromagnetic phase with a Curie temperature $T_{C1} \sim 11$ K. A weak remanent magnetic moment is observable above 11 K and persists at 300 K, indicating another ferromagnetic phase with a Curie temperature greater than 300 K. The magnetization is then measured when the sample is cooled back down. As can be seen in Fig. 3(a), there is a spontaneous magnetization at $B = 0$, which is only slightly lower than the remanent magnetization obtained in the scan with increasing temperature, suggesting that the low-temperature phase is predominantly single domain. Two mechanisms can lead to this behavior: (1) the high-temperature phase already present after the initial magnetization is capable of inducing the low-temperature phase during the process of cooling back down. (2) The low-temperature phase itself is spontaneous. To distinguish the two possibilities, we performed experiments with zero-field cooling (ZFC) on an as-grown sample, in which there was no magnetization from the high-temperature phase without prior applied field. When the temperature is lowered below 11 K, the magnetic moment appears and increases with decreasing temperature, indicating that the low-temperature ferromagnetic phase is spontaneous.

The hysteresis loops of the low-temperature phase show that the easy axis is perpendicular to the growth direction (in-plane), as can be seen from the in-plane and out-of-plane hysteresis loops shown in Fig. 3(b). An easy axis in the sample plane has also been observed in GaMnAs epilayers grown on GaAs buffers; the in-plane easy axis in this case is attributed to compressive strain [15]. The result on GaSb/Mn digital alloys grown on GaSb buffer layers is consistent with this interpretation, indicating that the observed ferromagnetism is hole induced, which is confirmed by the studies of dependence of ferromagnetism on applied electric bias.

However, depending on the growth conditions, the relative strength of the two phases varies, ranging from cases where only the high-temperature phase is observable to others for which only the low-temperature phase is present. Recently, we have succeeded in fabricating single-phase samples with T_C reaching 65–80 K (The obtained value of T_C depends on the measurement technique.), substantially higher than the T_C predicted for GaMnSb random alloys (~ 45 K) [16]. This improved T_C of the low-temperature phase in GaSb/Mn digital alloys is technologically important because it is close to liquid nitrogen temperature, and many GaSb/InAs-based devices for infrared applications operate at liquid nitrogen temperature [17,18]. The correlation between the structural and magnetic properties of these higher T_C samples is currently being investigated with the goal of further extending T_C.

Magnetotransport measurements reveal the interactions between charge carriers and magnetic ions, as in previous studies of magnetic semiconductors [5,19]. All samples exhibit metallic behavior, with the zero-field resistance only weakly dependent on temperature, rather than the exponentially thermally activated behavior observed in our studies of GaAs/Mn digital alloys [19]. The carrier densities estimated from the low-temperature and high-field region of the anomalous Hall effect (AHE) curves (data were taken up to 33 T at the NHMFL in Tallahassee) are between 18% and 50% of the nominal Mn concentration. This large hole density is important for the hole-mediated exchange interaction between Mn ions.

As discussed earlier, one of the most important properties of ferromagnetic semiconductors is the interaction between itinerant carriers and localized electron spins in Mn ions. The AHE provides information about the Mn-generated internal field experienced by itinerant carriers and the spin–orbit interaction of the carriers. The AHE first decreases with temperature but appears to recover and remains strong up to 400 K (data are shown in Fig. 4 for 4 and 400 K for simplicity) — the slope of the Hall resistance near zero field is a measure of the magnetization, as well as the strength of its coupling with the carriers. The sign of the AHE is related to the band structure of the itinerant carriers and the spin–orbit interaction [17]. We note that other possibilities, such as two carrier (electrons and holes) conduction, can also lead to behavior like that of Fig. 4. In our magnetotransport and magnetooptical studies, we observed both Shubnikov–de Hass oscillations and electron-active cyclotron resonance in some of the samples, although the samples are all dominantly p-type. The masses obtained from the two measurements are also close to that of the electron mass in GaSb. Electron-active cyclotron resonance, involving transitions between light and heavy hole bands, has recently been observed in p-type samples in extremely high fields [20]. In our case, however, the resonance was observed at low fields (~ 7 T), where

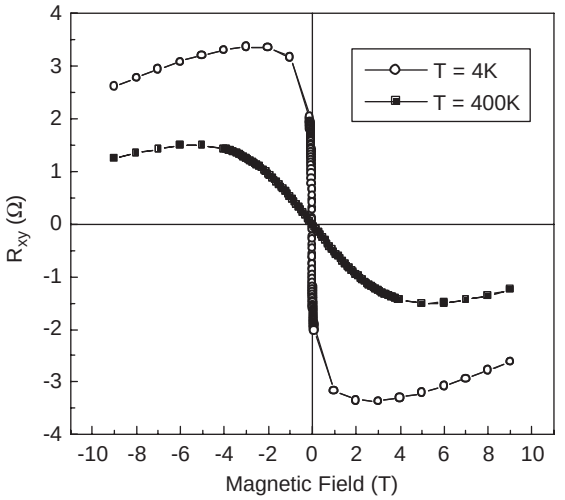

Fig. 4. The anomalous Hall effect of the sample shown in Fig. 1a.

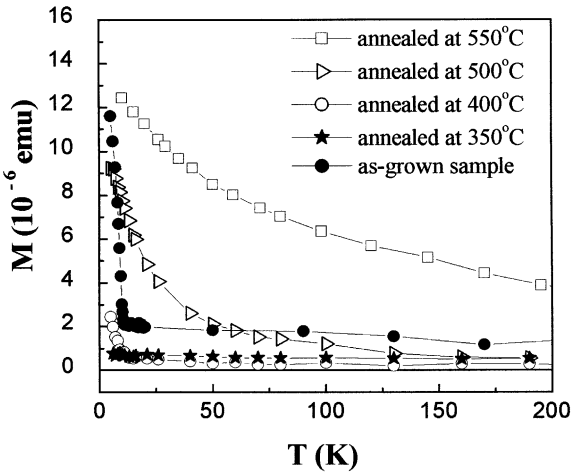

Fig. 5. The temperature dependences of remanent magnetization in a GaSb/Mn digital alloy annealed at the indicated temperatures.

such band structure effects are not expected to play a role. Therefore, we conclude that there are electrons in these samples (whose origin is uncertain). However, the electron densities and mobilities obtained from the cyclotron resonance data and Shubnikov–de Hass oscillations, combined with the hole densities determined from the high B low-temperature Hall effect data, do not reproduce (in a two-carrier model) the overall shape of the experimental curve shown in Fig. 4 at room temperature, particularly at low fields. However, it is clear that both the AHE and magnetoresistance curves are affected significantly by the presence of electrons.

As mentioned above, the AHE observed in low-temperature grown GaMnSb random alloys with no MnSb precipitates decreased rapidly above T_C (25 K), vanishing completely around 50 K. High-temperature grown GaMnSb samples containing 3D MnSb precipitates showed no clear AHE even at liquid helium temperature [14]. The AHE coefficient is found to be negative for the GaSb/Mn digital alloys at all temperatures, as for GaMnSb random alloys [5]. This is presently not understood. The AHE itself, even in extensively studied ferromagnetic metals, is not fully understood [21,22].

Based on the present results, we suggest the following picture. The Mn-containing layers consist of 2D GaMnSb random alloys (similar to 3D GaMnSb random alloys with randomly distributed Mn ions, but predominantly in and near the nominal Mn-containing planes) and 2D islands of zinc-blende MnSb, also predominantly in the Mn-containing planes. The low-temperature ferromagnetic phase is attributed to the isolated Mn portion (similar to GaMnSb random alloys). This can explain some similarities between the GaSb/Mn digital alloys and GaMnSb random alloys at low temperatures. The observed ferromagnetism at higher temperatures is associated with the 2D MnSb islands, which may be related to the high T_C found in bulk (NiAs structure) MnSb (580 K). A detailed theoretical study is needed to fully understand the mechanisms involved.

The temperature dependence of the remanent magnetic moment showed dramatic changes with annealing, even at rather low temperatures. Results for several samples from the same wafer annealed at different temperatures are shown in Fig. 5. Annealing at 250°C for up to 2 h did not result in any observable change in magnetic properties. After the sample was annealed at 350°C, however, the low-temperature phase disappeared and the magnetization became nearly temperature independent at a value less than half than seen in the unannealed sample above 11 K. As the annealing temperature increases, a new low-temperature ferromagnetic phase arises with increasing remanent magnetization, indicating changes in domain structures in the digital alloy, which is confirmed in the spontaneous magnetization measurements

discussed later. The sample annealed at 500°C for 5 min shows a remanent magnetic moment $\sim 1 \times 10^{-5}$ emu at 5 K (close to the remanent magnetic moment in the as-grown sample) and a Curie temperature estimated from Fig. 5 to be around 50 K. The sample annealed at 550°C shows a much higher Curie temperature with a correspondingly larger remanent magnetization at high temperatures. However, unlike GaMnSb epilayers grown at high substrate temperature with NiAs structure precipitates, which show nearly temperature independent hysteresis loops [14], the annealed samples have hysteresis loops that change rapidly as the temperature increases.

The annealing studies indicate that Mn atoms migrate within the structure at elevated temperatures. The magnetization studies also show that there are more possibilities than isolated Mn atoms and ZB MnSb quasi-2D islands. The low-temperature phase after annealing at 500°C does not behave in the same way as that in the as-grown sample. For example, there is no spontaneous magnetization for this low-temperature phase under ZFC conditions. It is possible that isolated Mn atoms coalesce into small structures within the digital layers, before merging with the larger ZB MnSb. Magnetization with zero-field cooling and the corresponding blocking temperature have been extensively used for studying properties of magnetic nanostructures, including particle sizes [23]. Our experimental and numerical studies clearly show an increase of island size with increasing annealing temperature. The details of results will be given elsewhere.

To further illustrate the changes with annealing, the coercive field at 5 K is plotted as a function of annealing temperature in Fig. 6. As can be seen, the change in coercive field is not monotonic with annealing temperature, indicating various possible structures forming and perhaps coalescing with increasing annealing temperature. The details of this evolution need to be investigated further.

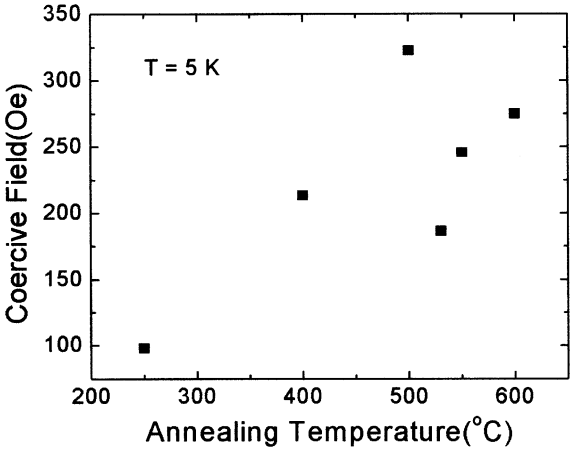

Fig. 6. The coercive field as a function of annealing temperature. The data point at 250°C (the growth temperature) was taken from the as-grown sample.

4. Dependence of ferromagnetism on applied electric bias

One key advantage of semiconductors for electronic applications is the relative ease with which carrier density can be modified by either applied electric bias or photoexcitation. Because the ferromagnetism of III-Mn-V materials is carrier (hole) mediated [24], it can be modified and controlled by suitable applied electric bias or in some cases by photoexcitation [25–27]. Although there has been an attempt to control ferromagnetism in (Ga,Mn)As and (Al,Ga,Mn)As by electric field, the experimental results showed that there was no observable electric field modulation of T_C or of the magnetization in these materials [28].

The effect of applied electric bias on ferromagnetism was studied for two GaSb/Mn digital alloy samples. The samples used showed similar behavior. We will present the result on the sample that showed a T_C of almost 80 K in magnetization measurements. The digital alloy consists of 50 repetitions of half monolayers (MLs) of Mn and 9 MLs of GaSb grown on AlSb and GaSb buffer layers. Hall bars with gate insulator (polyimide in this study) were fabricated, followed by making contact holes in the polyimide for source and drain. The electrical contacts for source and drain were formed by gold deposition, and Cr/Au was used as a gate metal contact. The magnetotransport measurements were performed in magnetic fields up to 9 T with a Hall sensor placed adjacent to the sample for in situ measurement of the applied magnetic field.

The ferromagnetism and its resulting hysteretic behavior observed in the Hall resistance are the most

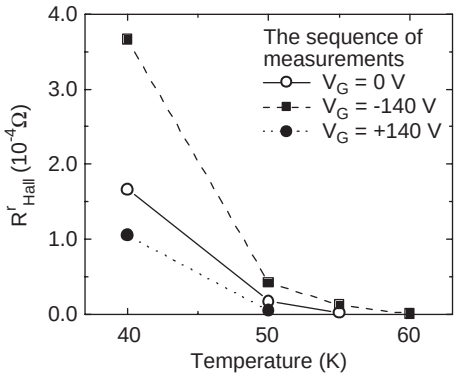

Fig. 7. Remanent Hall resistance (R^{r}_{Hall}) vs. temperature with different gate biases. The sequence of measurements follows the legends in the figure. The negative bias clearly increases the Curie temperature.

direct evidence of interaction between spins of itinerant carriers and localized electron spins in Mn ions. Changes in hole density should affect the magnetism. The application of a positive gate bias (gate electrode positive) should reduce the hole concentration, weakening the ferromagnetic order, while a negative bias should increase the hole concentration and enhance the ferromagnetic interaction among the Mn ions. A systematic study of the remanent Hall resistance (R^{r}_{Hall}, defined as R_{Hall} at $B=0$) as a function of the applied bias will provide information concerning the carrier-mediated ferromagnetism.

The applied gate bias was limited to ± 145 V to avoid dielectric breakdown of the insulator used in this study; higher V_G would, of course, result in a larger change of hole concentration. The expected change of sheet hole concentration from the gate capacitance of our structure is about 2×10^{12} cm^{-2} at a gate bias of ± 140 V. Fig. 7 shows the remanent Hall resistance (R^{r}_{Hall}) of the hysteresis loops in R_{Hall} as a function of temperature at ± 140 V bias and at zero/applied bias (before and after application of the bias). As can be seen, R^{r}_{Hall} changes systematically with electric bias, and is reproducible at zero applied bias. The sample is cycled to room temperature and back to the measurement temperature after each application of bias to liberate any trapped charge. Figures clearly shows that the ferromagnetism of the GaSb/Mn digital alloy can be switched on and off, depending on the direction and the magnitude of the applied bias.

5. Summary

In summary, GaSb/Mn digital alloys that show ferromagnetism above room temperature have been fabricated by MBE. Several microscopy techniques have been employed to characterize the materials. These studies show that the samples have good crystal quality with well-defined 2D Mn layers separated by GaSb layers, without 3D MnSb precipitates in the NiAs structure. The Mn layers themselves consist of MnSb islands and randomly distributed Mn ions, as revealed by XSTM images. These structural features are identified as sources of two ferromagnetic phases observed in some samples, both of which are ferromagnetic. In samples with a single (low temperature) phase, the Curie temperature has been raised to around liquid nitrogen temperature. Annealing studies showed that the low-temperature ferromagnetic phase in as-grown samples is very sensitive to annealing. It disappears after the sample is annealed at 350°C, and is replaced by another low-temperature phase with different magnetic properties after annealing at 400°C. Recent EXAFS studies of GaSb/Mn digital alloys, as-grown and annealed, indicate that Mn atoms remain bonded with the nearest-neighbor Sb atoms in the zinc-blende structure as long as the annealing temperature is below $\sim$ 500°C. Annealing at 550°C results in a transformation from the zinc-blende bonds to the NiAs bonds for the Mn atoms. We have demonstrated that ferromagnetism of GaSb/Mn digital alloy can be controlled by external electric field with the use of gated structure, which is a clear indication that the ferromagnetism in such digital alloys is carrier mediated.

Acknowledgements

This work was supported by the DARPA SPINS program through the Office of Naval Research under Grant ONR N00014-00-1-0951 and by NSF under Grant ECS0224206.

References

[1] H. Ohno, Science 291 (2001) 840.
[2] G.A. Prinz, Science 282 (1998) 1660.

[3] S. Koshihara, A. Oiwa, M. Hirasawa, S. Katsumoto, Y. Iye, C. Urano, H. Takagi, H. Munekata, Phys. Rev. Lett. 78 (24) (1997) 4617.
[4] A. Oiwa, A. Endo, S. Katsurnoto, Y. Iye, Phys. Rev. B 59 (8) (1999) 5826.
[5] F. Matsukura, E. Abe, H. Ohno, J. Appl. Phys. 87 (9) (2000) 6442.
[6] T. Dietl, H. Ohno, F. Matsukura, J. Cibert, D. Ferrand, Science 287 (2000) 1019.
[7] M.E. Overberg, C.R. Abernathy, S.J. Pearton, Appl. Phys. Lett. 79 (9) (2001) 1312.
[8] K. Ueda, H. Tabata, T. Kawai, Appl. Phys. Lett. 79 (7) (2001) 988.
[9] M.E. Overberg, B.P. Gila, G.T. Thaler, C.R. Abernathy, S.J. Pearton, N.A. Theodoropoulou, K.T. McCarthy, S.B. Arnason, A.F. Hebard, S.N.G. Chu, R.G. Wilson, J.M. Zavada, Y.D. Park, J. Vac. Sci. Technol. B 20 (2002) 969.
[10] Y. Matsumoto, M. Murakami, T. Shono, T. Hasegawa, T. Fukumura, M. Kawasaki, P. Ahmet, T. Chikyow, S. Koshihara, H. Koinuma, Science 291 (2001) 854.
[11] X. Chen, M. Na, M. Cheon, S. Wang, H. Luo, B.D. McCombe, X. Liu, Y. Sasaki, T. Wijtowicz, J.K. Furdyna, S.J. Potashnik, P. Schiffer, Appl. Phys. Lett. 81 (3) (2002) 551.
[12] M. Cheon, X. Chen, S. Wang, G.B. Kim, H. Luo, B.D. McCombe, G. Boishin, L.J. Whitman, X. Liu, Y. Sasaki, T. Wojtowicz, J.K. Furdyna, to be published.
[13] Y.L. Soo, Y.H. Kao, private communications.
[14] E. Abe, F. Matsukura, H. Yasuda, Y. Ohno, H. Ohno, Physica E 7 (2000) 981.
[15] H. Ohno, Science 281 (1998) 951.
[16] T. Dietl, H. Ohno, F. Matsukura, J. Cibert, D. Ferrand, Science 287 (2000) 1019.
[17] Y.-H. Zhang, R.H. Miles, D.H. Chow, IEEE J. Selected Topics Quantum Electron. 1 (1995) 749.
[18] T.H. Myers, et al., Appl. Phys. Lett. 61 (1992) 1816.
[19] H. Luo, B.D. McCombe, M.H. Na, K. Mooney, F. Lehmann, X. Chen, M. Cheon, S.M. Wang, Y. Sasaki, X. Liu, J.K. Furdyna, Physica E 12 (2002) 366.
[20] C.J. Stanton, private communication.
[21] T. Jungwirth, Q. Niu, A.H. MacDonald, cond-mat/0110484, 2001.
[22] J. Ye, Y.B. Kim, A.J. Millis, B.I. Shraiman, P. Majumdar, Z. Tesanovic, Phys. Rev. Lett. 83 (18) (1999) 3737.
[23] R. Coehoorn, C. Haas, R.A. de Groot, Phys. Rev. B 31 (1985) 1980.
[24] T. Dietl, H. Ohno, F. Matsukura, Phys. Rev. B 63 (2001) 195205.
[25] S. Koshihara, et al., Phys. Rev. Lett. 78 (1997) 4617.
[26] F. Matsukura, et al., Phyica E 12 (2002) 351.
[27] H. Ohno, et al., Nature 408 (2000) 944.
[28] D. Chiba, et al., J. Supercond. Novel Magn. 16 (2003) 179.